Guiding terahertz waves along subwavelength channels

A. I. Fernández-Domínguez,[1,*] Esteban Moreno,[1] L. Martín-Moreno,[2] and F. J. García-Vidal[1,†]
[1]*Departamento de Física Teórica de la Materia Condensada, Universidad Autónoma de Madrid, E-28049 Madrid, Spain*
[2]*Instituto de Ciencia de Materiales de Aragón (ICMA) and Departamento de Física de la Materia Condensada, CSIC–Universidad de Zaragoza, E-50009 Zaragoza, Spain*
(Received 6 November 2008; published 16 June 2009)

We propose a feasible way of guiding terahertz waves along V grooves whose lateral dimensions are subwavelength. A plasmonic metamaterial is built by periodically corrugating these channels in such a way that the system supports the propagation of electromagnetic modes with characteristics mimicking those of channel plasmon polaritons in the optical regime. These geometrically induced guided modes present long propagation lengths and low bending losses, making them excellent candidates for routing terahertz waves at planar surfaces.

DOI: 10.1103/PhysRevB.79.233104 PACS number(s): 42.79.Gn, 42.25.Bs, 73.20.Mf, 78.68.+m

Terahertz electromagnetic (EM) waves, with vacuum wavelengths typically ranging from 30 μm to 3 mm, have been less explored than those in the contiguous spectral regimes. Efficient sources and detectors of THz waves were lacking until recently, thus hindering the progress in this field. However, the numerous present and future applications for these waves, such as time-domain spectroscopy,[1] biomedical[2] and security[3] imagings, and ultrahigh speed electronics, together with advances in their generation and detection have triggered the interest in THz signal routing systems.[4] Sommerfeld showed more than 100 years ago that EM modes supported by metallic wires can be used for guiding radiation for very low frequencies.[5,6] These Sommerfeld waves are mathematically identical to the surface-plasmon polaritons (SPPs) occurring in the visible regime but, due to the contrasting values of the permittivity of metals in the THz and visible regimes, their physical properties are very different. In comparison to SPPs in the visible regime, absorption of THz-SPPs is very low, but they are very poorly confined making them unsuitable for routing applications.

In this Brief Report we present a guiding scheme to achieve subwavelength transverse confinement of THz waves at a planar surface. The design, which consists of corrugated V grooves milled on a metal surface, borrows ideas from channel plasmon polaritons (CPPs) in the visible range[7] and the concept of geometrically induced SPPs.[8] The combination of these two different basic mechanisms allows overcoming the aforementioned limitations of THz wave routing. We study both the guiding properties of straight waveguides and the bending losses, present in any nontrivial circuit. While keeping long mode propagation, good confinement and reasonable bending loss for radii of curvature of the order of a few wavelengths are demonstrated, making these waveguides interesting in the aforementioned context.

In the visible or telecom regimes, V-shaped grooves milled in metals support low loss, tightly confined CPPs.[9–11] The modal size of CPPs grows for increasing wavelength in such a way that, on perfect electrical conductors (PECs), a good approximation at THz frequencies, CPPs do not exist. An interesting way to overcome this limitation is by taking advantage of the geometrically induced surface EM modes, also termed spoof SPPs, that emerge when a PEC surface is periodically corrugated.[8,12–15] We will now test whether corrugated V grooves milled on a PEC surface sustain EM guided modes. For that, we analyze first the dependence of the EM modes propagating in the gap between two parallel groove arrays (see lower inset of Fig. 1) on the gap width, w. Similar modes supported in the gap between two metallic surfaces textured with two-dimensional (2D) hole arrays have been considered in the GHz regime.[16] Here we only consider EM modes associated with longitudinal electric fields having odd parity with respect to the gap center because they have the same symmetry properties as the CPPs at optical frequencies.[17] In the very subwavelength regime, with the wavelength, λ, being much larger than the period of the array, d, and the width of the grooves, a, it is straightforward to calculate the dispersion relation (frequency versus momentum, k) of these EM guided modes

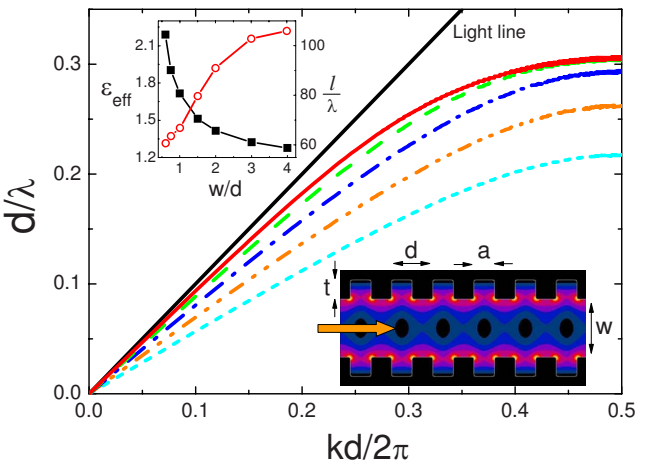

FIG. 1. (Color online) Dispersion relation of the guided EM modes propagating between two corrugated PEC surfaces. Both surfaces are identical and consist of two rectangular groove arrays of period d. The grooves width a and depth t are equal to $0.5d$. Five different gap widths (w) are considered: $4d$ (red solid line), $2d$ (green dashed line), d (blue dotted dashed line), $0.5d$ (orange double dotted dashed line), and $0.25d$ (cyan dotted line). In the lower inset, the electric field amplitude at the band edge for the case $w=1.5d$ is depicted. The upper inset renders ϵ_{eff} (black squares) and the propagation length (red circles) at $d/\lambda=0.25$ obtained within the SIBC approximation for Al and $d=200$ μm.

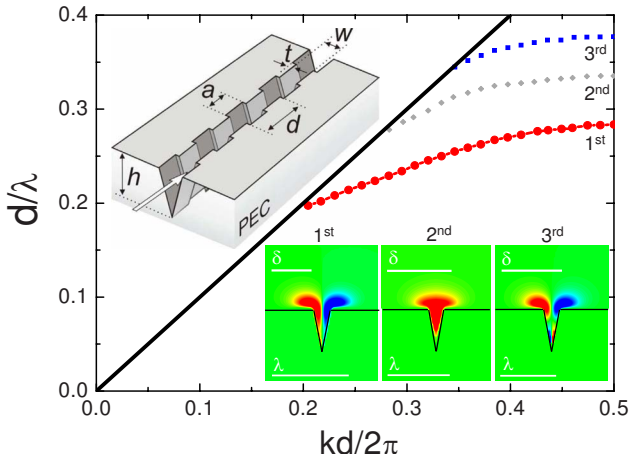

FIG. 2. (Color online) FDTD dispersion relation of the first three spoof CPP modes supported by a corrugated V channel milled on a PEC surface. A schematic picture of the structure is shown in the upper inset. Lower insets depict the amplitudes of the longitudinal component of the electric field evaluated at the band edge for the three modes. The wavelength, λ, and modal size, δ, for the three cases are represented.

$$\frac{\sqrt{k^2-k_0^2}}{k_0}\coth\left(\sqrt{k^2-k_0^2}\frac{w}{2}\right)=S_0^2\tan(k_0t), \tag{1}$$

where t is the depth of the grooves, $k_0=\frac{2\pi}{\lambda}$, and $S_0=\sqrt{\frac{a}{d}}\,\mathrm{sinc}(k\frac{a}{2})$. Equation (1) resembles the dispersion relation of the antisymmetric gap SPP modes supported in a dielectric slab sandwiched between two semi-infinite metals.[18] Figure 1 renders the dispersion relation of the gap modes traveling between two identical groove arrays. These results have been computed with a modal expansion technique including a sufficiently large number of modes to achieve convergence. In all cases, the geometrical parameters of the grooves are $t=a=0.5d$. Note that, as we are considering PEC boundary conditions, all magnitudes are scalable and we can take the period d as the unit length. Structures with five different gap widths have been analyzed, ranging from $w=4d$ to $w=0.25d$. Importantly, the dispersion bands are lowered as w is reduced. Thus, for a given frequency, k is larger for smaller w. This effect can be quantified by looking at the effective permittivity of the mode, ϵ_{eff} (defined as $\epsilon_{\mathrm{eff}}=k^2/k_0^2$). In the upper inset of Fig. 1, ϵ_{eff} of the gap modes at $d/\lambda=0.25$ as a function of w is shown. For decreasing values of w, ϵ_{eff} increases very rapidly, reflecting a very large lateral confinement of the mode as the gap is reduced.

The existence of EM guided modes in the gap between two corrugated PEC surfaces and the dependence of ϵ_{eff} with the gap width suggest that a corrugated V groove milled on a PEC film (see upper inset of Fig. 2) would support the propagation of EM guided modes. These will be tightly confined in the transverse plane and localized at the bottom of the groove, where ϵ_{eff} is maximum. In order to verify this hypothesis, we have carried out finite difference time domain (FDTD) calculations of the dispersion relation of the EM modes supported by corrugated V grooves. As in the previous calculations, we assume that the metal behaves as a PEC, i.e., no absorption is present in the structure. The geometrical parameters are $a=t=0.5d$, $w=0.76d$, and $h=5d$, corresponding to a groove angle of 20°. The bands associated with the first three EM guided modes (spoof CPPs) traveling along the corrugated channel are rendered in Fig. 2. The fact that the corrugated V channel has a finite height translates into the existence of a cutoff for these EM guided modes.

In contrast to other THz waveguiding schemes,[19] the spoof CPPs presented here have sub-λ transverse modal size. The longitudinal components of the electric field associated with them are shown in the lower insets of Fig. 2. The fields are evaluated at the band edges of the three dispersion bands. Electric fields are plotted only inside the shallow part of the corrugated V channel, where the modes are strongly localized. The first and third modes have odd parity, as the longitudinal electric fields for these modes have a different sign at both sides of the V channel, vanishing at the middle plane. The lowest mode shows only two lobes, whereas the third one presents another plane, now parallel to the planar surface, in which the longitudinal electric field is zero. The second EM guided mode has even parity with respect to the symmetry plane. In all three insets, both λ and the modal size, δ, are represented. This modal size is (arbitrarily) defined as the transverse separation between the locations where the electric field amplitude has fallen to one tenth of its maximum value, being $\delta=0.52\lambda$, 1.02λ, and 1.06λ for these three modes at their band edges. Another interesting feature of the modal shape of these propagating modes is that, contrary to what the behavior of ϵ_{eff} predicts, the modes are not guided at the groove bottom but rather at the groove edges. This is due to their strong hybridization with wedge modes that run on the edges of the groove, much in the same way as it occurs in the telecom regime.[17] The fact that the frequency overlap of the first and second bands is very small facilitates the monomode operation of this corrugated V groove as a THz waveguide. Notice that this single-mode characteristic has been achieved thanks to an appropriate election of the geometrical parameters.

Once we have demonstrated that indeed spoof CPPs are supported by infinitely long corrugated V grooves, it is worth analyzing how these EM modes behave in waveguides of finite length. For that, we have performed extensive numerical simulations of finite corrugated V channels using the CST MICROWAVE STUDIO™ software implementing the finite integration technique. As in the previous FDTD calculations, we also consider PEC boundary conditions. We have chosen the structure period $d=200$ μm, keeping the relation between the rest of the geometrical parameters and d as in the FDTD calculations reported in Fig. 2. First, in order to cross-check the different numerical techniques, we analyze the case of a straight channel. The channel is 20 mm long and the structure is illuminated from one end with a 2D input port mode that tries to resemble the spatial and vectorial dependencies of the lowest spoof CPP mode as obtained from FDTD simulations.

Within FIT it is possible to calculate the EM transmission through the finite waveguide by integrating the longitudinal component of the Poynting vector in two perpendicular planes located near the input and exit sides of the waveguide.

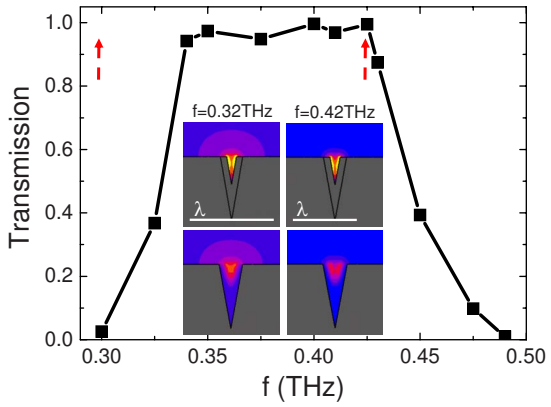

FIG. 3. (Color online) FIT simulations of the transmittance spectrum for the lower spoof CPP mode supported by a straight corrugated PEC V channel of period $d=200$ μm and total length 20 mm. Red dashed arrows indicate the spectral position of the cutoff and band-edge frequencies obtained from FDTD calculations. The left insets show the electric field amplitude at 0.32 THz and the right ones at 0.42 THz. Upper (lower) insets correspond to the plane located 9.1 mm (9.2 mm) away from the illuminated end of the structure.

Figure 3 shows this FIT transmission spectrum for the finite-length channel described above. Red dashed arrows indicate the cutoff and band-edge frequencies predicted by the FDTD method (see Fig. 2) for the lowest guided mode supported by the structure. The agreement between the two distinct numerical techniques in the spectral location of the band edge is excellent. Regarding the cutoff frequency, FIT predicts a slightly higher location than that obtained with FDTD. Notice that, as the band approaches its cutoff frequency, the spoof CPP mode becomes less localized and both numerical calculations are less accurate due to the inherent finite size of their spatial simulation windows. The important point is that the transmission approaches unity within the spectral region in which the lowest guided mode is supported. The insets of Fig. 3 show the total electric field amplitudes at two different frequencies. Left panels are evaluated at 0.32 THz and the right ones at 0.42 THz. The upper insets depict the electric field in the plane located 9.1 mm away from the illuminated end of the structure and correspond to the shallow part of the V channel. The lower insets are displaced one half of the period, then showing the deepest region in the groove. In accordance with the FDTD calculations, the electric field is strongly confined within the shallow channel. The insets also show clearly how the lateral confinement of the mode is much higher at 0.42 THz ($\delta=0.42$ mm$=0.59\lambda$) than at 0.32 THz ($\delta=1.37$ mm$=1.46\lambda$).

In all the previous calculations, as we were assuming ideal PEC boundary conditions, the modal propagation length, l, is infinite. One way to estimate l in a *real* waveguide operating at THz frequencies is by looking at the dependence of l with the gap width for the EM modes propagating in the region between two corrugated surfaces (see Fig. 1). In order to take into account the losses experienced by the EM fields propagating on such structures, it is possible to exchange PEC conditions by the so-called surface impedance boundary conditions (SIBCs).[20] In the upper inset

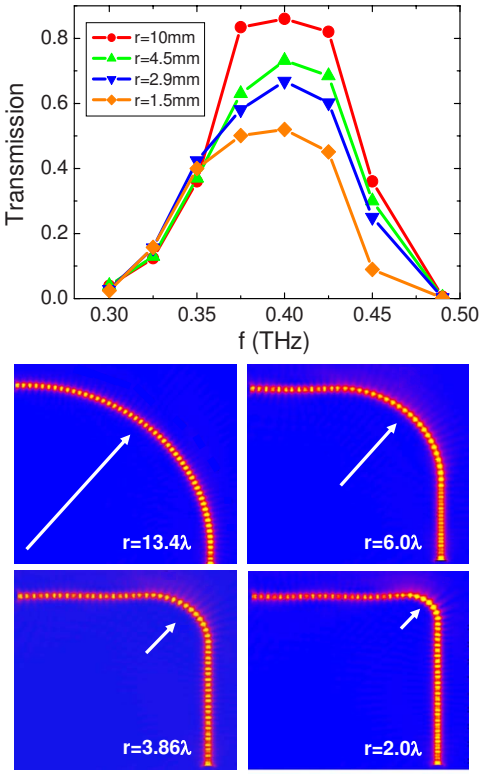

FIG. 4. (Color online) FIT simulations of the mode propagation through four 90° bend channels of different r. All structures are comprised by 100 periods. Upper panel renders the transmission spectrum for the four channels considered. Lower panels show the electric field amplitude at 0.40 THz evaluated at a height of 100 μm above the planar surface for the four structures analyzed.

of Fig. 1, the dependence of l (defined as $l=[2\ \mathrm{Im}(k)]^{-1}$) with w is displayed (red circles). For these calculations, we have fixed a frequency of 0.38 THz (the center of the transmission plateau in Fig. 3) and we have assumed that the metal is aluminum, taking its permittivity from Ref. 21. The evolution of l with w shows that there is a tradeoff between the propagation length and the transverse confinement of the EM guided mode, as is common in plasmonic structures. For example, for a width of $0.76d$ (as the opening of the V grooves analyzed in Figs. 2 and 3), l is of the order of 60λ. Similar estimations are obtained from three-dimensional (3D)-FIT simulations on straight corrugated aluminum V channels that incorporate absorption losses within the metal. Notice that this propagation length is much larger than those reported for other THz waveguiding schemes.[4,22]

When thinking in the possible use of spoof CPPs for routing THz radiation in planar surfaces, the question on the bending losses naturally arises. We have performed FIT simulations on corrugated bend V grooves milled on PEC surfaces (in order to isolate bending losses from the absorption losses previously discussed). The results obtained for four different 90° bends with different radii of curvature, r, are shown in Fig. 4. In all cases, the structures contain up to 100 periods. The groove array period in the straight part of the channel is equal to 200 μm and is slightly adjusted in the bends in order to conform with the curved geometry. The transmittance spectra for the four structures analyzed are

shown in the upper panel of Fig. 4. For the case of maximum r (10 mm), the transmission can be as large as 90%, but is reduced as r becomes smaller, being 50% in the case in which r is 1.5 mm (around 2 times the wavelength). These bending losses are much smaller than those reported for metallic wires at THz frequencies,[23] as expected due to the subwavelength character of the spoof CPPs. In the four lower panels of Fig. 4, the electric field amplitude evaluated at 0.40 THz in a plane located 100 μm above the planar surface is depicted. It is clear how the bending losses in these structures stem from radiation into vacuum modes occurring just at the bend of the waveguide. Notice that no attempt to reduce these losses by optimizing the geometry of the bend has been performed.

In conclusion, we have proposed a guiding mechanism for THz EM fields featuring subwavelength transverse confinement and valid for metallic planar geometries. The guided mode sustained by the V groove is induced geometrically, owing its existence to the periodic corrugation of the surface. Its tight confinement is due to the increased coupling between the fields supported at both sides of the groove. In addition to reduced modal sizes, such waveguides display long propagation lengths and low bending losses, being very promising for applications that require THz waves routing.

This work was sponsored by the Spanish Ministry of Science under Projects No. MAT2005-06608-C02 and No. CSD2007-046-NanoLight.es.

*anisaac.fernandez@uam.es
†fj.garcia@uam.es

[1] J. Zhang and D. Grischkowsky, Opt. Lett. **29**, 1617 (2004).
[2] M. Nagel, P. Haring Bolivar, M. Brucherseifer, H. Kurz, A. Bosserhoff, and R. Büttner, Appl. Phys. Lett. **80**, 154 (2002).
[3] J. F. Federici, B. Schulkin, F. Huang, D. Gary, R. Barat, F. Oliveira, and D. Zimdars, Semicond. Sci. Technol. **20**, S266 (2005).
[4] A. Ishikawa, S. Zhang, D. A. Genov, G. Bartal, and X. Zhang, Phys. Rev. Lett. **102**, 043904 (2009).
[5] A. Sommerfeld, Ann. Phys. Chem. **67**, 233 (1899).
[6] K. Wang and D. M. Mittleman, Nature (London) **432**, 376 (2004).
[7] I. V. Novikov and A. A. Maradudin, Phys. Rev. B **66**, 035403 (2002).
[8] J. B. Pendry, L. Martín-Moreno, and F. J. García-Vidal, Science **305**, 847 (2004); F. J. García-Vidal, L. Martín-Moreno, and J. B. Pendry, J. Opt. A, Pure Appl. Opt. **7**, S97 (2005).
[9] D. F. P. Pile and D. K. Gramotnev, Opt. Lett. **29**, 1069 (2004); **30**, 1186 (2005).
[10] S. I. Bozhevolnyi, V. S. Volkov, E. Devaux, and T. W. Ebbesen, Phys. Rev. Lett. **95**, 046802 (2005).
[11] S. I. Bozhevolnyi, V. S. Volkov, E. Devaux, J.-Y. Laluet, and T. W. Ebbesen, Nature (London) **440**, 508 (2006).
[12] A. P. Hibbins, B. R. Evans, and J. R. Sambles, Science **308**, 670 (2005).
[13] S. A. Maier, S. R. Andrews, L. Martín-Moreno, and F. J. García-Vidal, Phys. Rev. Lett. **97**, 176805 (2006).
[14] C. R. Williams, S. R. Andrews, S. A. Maier, A. I. Fernández-Domínguez, L. Martín-Moreno, and F. J. García-Vidal, Nat. Photonics **2**, 175 (2008).
[15] Q. Gan, Z. Fu, Y. J. Ding, and F. J. Bartoli, Phys. Rev. Lett. **100**, 256803 (2008).
[16] A. P. Hibbins, M. J. Lockyear, and J. R. Sambles, Phys. Rev. B **76**, 165431 (2007).
[17] E. Moreno, F. J. García-Vidal, S. G. Rodrigo, L. Martín-Moreno, and S. I. Bozhevolnyi, Opt. Lett. **31**, 3447 (2006).
[18] E. N. Economou, Phys. Rev. **182**, 539 (1969).
[19] W. Zhu, A. Agrawal, and A. Nahata, Opt. Express **16**, 6216 (2008).
[20] J. D. Jackson, *Classical Electrodynamics*, 2nd ed. (Wiley, New York, 1975).
[21] M. A. Ordal, L. L. Long, R. J. Bell, S. E. Bell, R. R. Bell, R. W. Alexander, Jr., and C. A. Ward, Appl. Opt. **22**, 1099 (1983).
[22] A. A. Govyadinov and V. A. Podolskiy, Phys. Rev. B **73**, 155108 (2006).
[23] K. Wang and D. M. Mittleman, J. Opt. Soc. Am. B **22**, 2001 (2005).

CST视频培训课程推荐

CST 微波工作室(CST Microwave Studio)是 CST 工作室套装中最核心的一个子软件，主要用于三维电磁问题的仿真分析，可计算任意结构任意材料电大宽带的电磁问题。广泛应用于高频/微波无源器件的仿真设计、各种类型的天线设计、雷达散射截面分析、电磁兼容分析和信号完整性分析等各个方面。

易迪拓培训(www.edatop.com)推出的 CST 微波工作室视频培训课程由经验丰富的专家授课，旨在帮助用户能够快速地学习掌握 CST 微波工作室的各项功能、使用操作和工程应用。购买 CST 教学视频培训课程套装，还可超值赠送 3 个月免费在线学习答疑，让您学习无忧。

CST 学习培训课程套装

该培训套装由易迪拓培训联合微波 EDA 网共同推出，是最全面、系统、专业的 CST 微波工作室培训课程套装，所有课程都由经验丰富的专家授课，视频教学，可以帮助您从零开始，全面系统地学习 CST 微波工作的各项功能及其在微波射频、天线设计等领域的设计应用。且购买该套装，还可超值赠送 3 个月免费学习答疑…

课程网址：http://www.edatop.com/peixun/cst/24.html

HFSS 天线设计培训课程套装

套装共含 5 门视频培训课程，课程从基础讲起，内容由浅入深，理论介绍和实际操作讲解相结合，全面系统的讲解了 CST 微波工作室天线设计的全过程。是国内最全面、最专业的 CST 天线设计课程，可以帮助您快速学习掌握如何使用 CST 设计天线，让天线设计不再难…

课程网址：http://www.edatop.com/peixun/cst/127.html

更多 CST 视频培训课程：

- **CST 微波工作室入门与应用详解 — 中文视频教程**
  CST 微波工作室初学者的最佳培训课程，由工程经验丰富的资深专家授课，全程中文讲解，高清视频，直观易学。网址：http://www.edatop.com/peixun/cst/25.html
- **CST 微波工作室天线设计详解 — 中文视频培训教程**
  重点讲解天线设计相关知识和使用 CST 进行天线仿真设计的使用操作，是学习掌握使用 CST 微波工作室进行天线设计的必备课程，网址：http://www.edatop.com/peixun/cst/26.html
- **CST 阵列天线仿真设计实例详解 —— 中文视频教程**
  阵列天线设计专业性要求很高，因此相关培训课程是少之又少，该门培训课程由易迪拓培训重金聘请专家讲解；课程网址：http://www.edatop.com/peixun/cst/123.html
- **更多 CST 培训课程**，敬请浏览：http://www.edatop.com/peixun/cst

关于易迪拓培训：

易迪拓培训(www.edatop.com)由数名来自于研发第一线的资深工程师发起成立，一直致力和专注于微波、射频、天线设计研发人才的培养；后于 2006 年整合合并微波 EDA 网(www.mweda.com)，现已发展成为国内最大的微波射频和天线设计人才培养基地，成功推出多套微波射频以及天线设计相关培训课程和 ADS、HFSS 等专业软件使用培训课程，广受客户好评；并先后与人民邮电出版社、电子工业出版社合作出版了多本专业图书，帮助数万名工程师提升了专业技术能力。客户遍布中兴通讯、研通高频、埃威航电、国人通信等多家国内知名公司，以及台湾工业技术研究院、永业科技、全一电子等多家台湾地区企业。

我们的课程优势：

※ 成立于 2004 年，10 多年丰富的行业经验

※ 一直专注于微波射频和天线设计工程师的培养，更了解该行业对人才的要求

※ 视频课程、既能达到现场培训的效果，又能免除您舟车劳顿的辛苦，学习工作两不误

※ 经验丰富的一线资深工程师讲授，结合实际工程案例，直观、实用、易学

联系我们：

※ 易迪拓培训官网：http://www.edatop.com

※ 微波 EDA 网：http://www.mweda.com

※ 官方淘宝店：http://shop36920890.taobao.com